Point-source atom interferometer gyroscope(*)

Azure Hansen, Yun-Jhih Chen, John E. Kitching and Elizabeth A. Donley

Time and Frequency Division, National Institute of Standards and Technology
325 Broadway, Boulder, CO 80305 USA

Summary. — Point-source atom interferometry (PSI) with cold atoms in a centimeter-scale vacuum cell has applications in inertial navigation. PSI uses light pulses in a Raman configuration to interfere atomic wavepackets in an expanding cloud of laser-cooled atoms. The measurement is inherently multi-axis in a single experimental run, measuring the component of the rotation vector of the system in the plane perpendicular to the Raman beam axis and the acceleration along that axis. A key difference between PSI and conventional atom interferometry is that instead of minimizing the thermal expansion of the cold-atom cloud, PSI exploits the expansion to probe these three quantities simultaneously.

1. – Introduction

Light pulse atom interferometry [1, 2] enables inertial measurements of acceleration and rotation. Recent research includes building both extremely sensitive meter-scale laboratory experiments to study gravitation [3-5] and portable instruments for field measurements [6-10]. Our work explores the potential for a particular technique, point-source

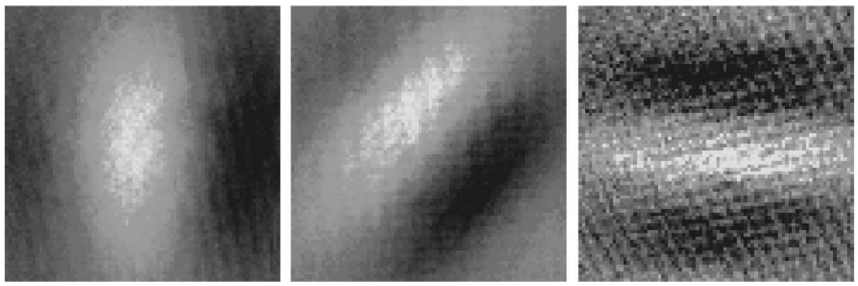

Fig. 1. – Interference fringe data generated by a simulated rotation. The atom fringe orientation measures the system rotation direction; the fringe period measures the system rotation magnitude. Left: $\Omega_y = 35\,\mathrm{mrad/s}$. Center: $\Omega_x = \Omega_y = 25\,\mathrm{mrad/s}$. Right: $\Omega_x = 89\,\mathrm{mrad/s}$.

atom interferometry (PSI) with cold atoms [11, 12], to be used as an inertial sensor for navigation [13-15]. PSI has a number of inherent advantages over other atom interferometer gyroscope approaches, including multi-axis sensitivity, a non-ambiguous rotation measurement, and a simplified experimental apparatus.

By using an expanding cloud of cold atoms with the Mach-Zehnder optical Raman pulse sequence, PSI generates spatially-resolved interference fringes that measure two axes of rotation and one of acceleration [11-14]. Each atom interferes only with itself; this parallelism combined with position-velocity correlation creates a wavefunction phase gradient across the cloud that depends on the inertial motion of the system. The fringe orientation measures the orientation of the rotation vector projected onto the plane perpendicular to the Raman beams, the fringe spatial frequency measures the rotation magnitude in that plane, and the fringe phase offset measures the acceleration along the Raman beam axis (see fig. 1). These three quantities are obtained in a single run of the experiment with a single cloud of cold atoms and are easily differentiated from each other.

During the $\frac{\pi}{2}$-π-$\frac{\pi}{2}$ Mach-Zehnder pulse sequence [1, 2], the interferometer phase shift acquired due to inertial forces is given by $\Phi(\mathbf{r}) = \Phi_{\mathbf{a}} + \Phi_{\mathbf{\Omega}} + \Phi_{\mathrm{L}}$, where $\mathbf{k}_{\mathrm{eff}}$ is the effective Raman wavevector, $\mathbf{a}$ is the acceleration of the system, T is the Ramsey time between Raman pulse pairs, $\mathbf{k}_\Omega$ is the phase gradient due to rotation, and Φ_{L} is the laser phase. The first term is from a homogeneous acceleration, $\Phi_{\mathbf{a}} = \mathbf{k}_{\mathrm{eff}} \cdot \mathbf{a}T^2$, and the second is the spatial phase gradient from the system rotation, $\Phi_\Omega = \mathbf{k}_\Omega \cdot \mathbf{r}$. The rotation phase gradient is given by $\mathbf{k}_\Omega = (\mathbf{k}_{\mathrm{eff}} \times \mathbf{\Omega}) 2T^2/T_{\mathrm{ex}}$, where $\mathbf{\Omega}$ is the rotation of the system and T_{ex} is the expansion time of the cloud. The probability for an atom to be in the excited state after the interferometer sequence is given by $P(\mathbf{r}) = \frac{1}{2}(1 - C\cos\Phi(\mathbf{r}))$, where C is the interferometer fringe contrast.

The sensitivity of the gyroscope to rotation depends on the oriented area enclosed during the interferometer sequence, $\mathbf{A} = \mathbf{v}_0 T \times \mathbf{v}_r T$, where $\mathbf{v}_0$ is the initial atom velocity and $\mathbf{v}_r = h\mathbf{k}_{\mathrm{eff}}$ is the atom recoil velocity. The rotation phase can therefore also be written as $\Phi_{\mathbf{\Omega}} = \frac{2m}{\hbar}\mathbf{\Omega} \cdot \mathbf{A}$.

In point-source atom interferometry, the initial transverse velocity distribution in the

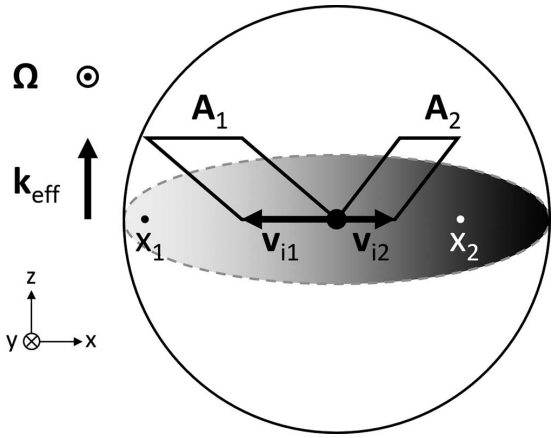

Fig. 2. – The origin of the two-dimensional sensitivity in point-source atom interferometry. As the cold-atom cloud (illustrated by the sphere) expands, two representative atoms move out from its center. Their initial velocities projected onto the xy-plane are $\mathbf{v}_{i1} = -v_{i1}\hat{x}$ and $\mathbf{v}_{i2} = v_{i2}\hat{x}$; it is only this component that contributes to the PSI measurement. The co-linear counter-propagating Raman beam pair is applied along the z-axis and transfers linear momentum $\mathbf{k}_{\text{eff}} = k_{\text{eff}}\hat{z}$ to each atom. During the Raman interrogation sequence, the atom superposition encloses a parallelogram with oriented area $\mathbf{A}_1$ or $\mathbf{A}_2$. The final position x_1 or x_2 of the atom depends on its initial velocity as $\mathbf{x} = \mathbf{v}_i T_{\text{ex}}$, preserving the phase information in a spatial phase map. The spatial phase distribution is indicated here by a gradient; its orientation and magnitude measures the system rotation vector $\mathbf{\Omega}$ projected into the xy-plane.

cold-atom cloud leads to a distribution in the area enclosed by each atom during the interferometer interrogation sequence [11-14]. At the end of the measurement, the position-velocity correlation at each point preserves the accumulation of the phases from every atom, creating a spatial phase map $\Phi(\mathbf{r})$ and, by the equation for $P(\mathbf{r})$, spatially-resolved spin state fringes. Each of these simultaneous, independent single-atom interferometers is sensitive to rotation orthogonal to its oriented area, which depends on its initial velocity and the momentum imparted by the Raman interaction (see fig. 2).

With the atom cloud expanding radially in all directions, the symmetry of the light-matter interaction and the parallelism of PSI makes it inherently sensitive to rotation in two dimensions: the projection of the rotation vector into the plane perpendicular to the optical Raman beam axis. The spatial phase gradient $\mathrm{d}\Phi_\Omega/\mathrm{d}v = 2k_{\text{eff}}T^2\Omega$ is measured and the value obtained for $|\mathbf{\Omega}|$ unambiguous [15]. This is in contrast to non-PSI gyroscopes where the atom population signal is integrated over the cloud onto a photodiode, making the measured phase Φ_Ω ambiguous to an unknown multiple of 2π [2]. However, all atom interferometer measurements of acceleration have a 2π ambiguity [7, 15]. Such ambiguities are resolved with additional measurements, reducing bandwidth and/or sensitivity [2, 7].

2. – Performance

In our current configuration, the measured sensitivities for the magnitude and direction of the applied rotation vector are $0.033\,^\circ/\mathrm{s}$ and 0.27°, respectively, for 1 s averaging time [14]. Our estimates of the shot-noise-limited performance for an ideal point-source gyroscope with the same parameters are $1 \times 10^{-4}\,^\circ/\mathrm{s}$ and $3 \times 10^{-3}\,^\circ$ at 1 s [14]. The fractional acceleration sensitivity is $\delta g/g = 1.6 \times 10^{-5}/\sqrt{\mathrm{Hz}}$ [14]. The performance of this system is limited by a number of effects, including the interrogation time of the optical Raman sequence ($T = 8\,\mathrm{ms}$), the atom cloud not being an ideal point source, the dead time of the experiment, the Raman laser phase noise (90 mrad at 1 s), and the vibrations of the Raman optics (62 mrad at 1 s) [13, 14, 16, 17].

Compact instruments have intrinsic challenges and trade-offs that we are working to further understand, overcome, and balance. A compact PSI system typically operates outside of the point-source limit: the final cloud size is only a few times larger than the initial cloud size [11-14]. This can be modeled as the convolution of a point source and the finite initial cloud size [13]. The gyroscope scale factor, relating the measured to the actual rotation, is therefore modified as $\Omega_{\mathrm{measured}} = \Omega_{\mathrm{actual}}(1 - \sigma_0^2/\sigma_f^2)$, where σ_0 and σ_f are the initial and final cloud waists, respectively [13]. The maximum fringe contrast is reduced as $C = C_0 \exp[-\frac{1}{2}\frac{k_\Omega^2 \sigma_i^2}{(1-\sigma_i^2/\sigma_f^2)}]$, where C_0 is the contrast for an ideal point source [13].

Rotation stability measurements in our system indicate that the dominant source of noise is from fluctuations in the initial cloud shape and size, which lead to fluctuations in the scale factor and therefore limit the sensitivity of our instrument. We are pursuing multiple approaches for mitigating, compensating for, and eliminating these effects [18].

We have developed a new measurement and analysis method to support these efforts: Simple, High dynamic range, and Efficient Extraction of Phase map (SHEEP) [15]. It is analogous to optical phase-shifting interferometry [19, 20], highlighting the potential for atom optics to benefit from established techniques in optics. Four atomic fringe images, shifted in phase from one to the next by $\pi/2$ by adjusting the Raman detuning chirp rate, are used to directly calculate the spatially-dependent atom phase map. By stepping through four values of Φ_L, each pixel in the fringe image traces out the sinusoidal variation in the atomic population, eliminating the need for fitting. The phase map is given by

$$\phi(x_i, y_j) = \arctan \frac{P_2(x_i, y_j) - P_4(x_i, y_j)}{P_3(x_i, y_j) - P_1(x_i, y_j)} + n\pi,$$

where P_L is the intensity value at each pixel at point (x_i, y_j) for the $L = 1 \ldots 4$ phase-shifted images and n is an integer [15]. Because the phase map is calculated pixel by pixel and no fitting is required, the minimum resolvable rotation rate is smaller than for other analysis methods [15]. While the bandwidth of our compact PSI system is primarily limited by the cold-atom loading time, the SHEEP method enables higher inertial measurement rates [15].

3. – Conclusion

Point-source atom interferometry has potential for applications requiring a portable science package. We have measured the sensitivity of our centimeter-scale science package and are further characterizing and optimizing the system and protocols for use as an inertial quantum sensor.

* * *

We thank M. A. Kasevich for helpful discussions and R. Boudot, G. W. Hoth, E. Ivanov, B. Pelle, S. Riedl, and M. Shuker for experimental contributions. A. H. was supported under an NRC Research Associateship award at NIST. This work was funded by NIST, a United States government agency, and it is not subject to copyright.

REFERENCES

[1] Kasevich M. and Chu S., *Phys. Rev. Lett.*, **67** (1991) 181.
[2] Tino G. M. and Kasevich M. A. (Editors), *Proceedings of the International School of Physics "Enrico Fermi,"* Course 188, *"Atom Interferometry"* (SIF, Bologna and IOS Press, Amsterdam) 2014.
[3] Rosi G., Sorrentino F., Cacciapuoti L., Prevedelli M. and Tino G. M., *Nature*, **510** (2014) 518.
[4] Hamilton P., Jaffe M., Haslinger P., Simmons Q., Müller H. and Koury J., *Science*, **349** (2015) 849.
[5] Canuel B. *et al.*, *Sci. Rep.*, **8** (2018) 14064.
[6] Barrett B., Antoni-Micollier L., Chichet L., Battelier B., Lévèque T., Landragin A. and Bouyer P., *Nat. Commun.*, **7** (2016) 13786.
[7] Freier C., Hauth M., Schkolnik V., Leykauf B., Schilling M., Wziontek H., Scherneck H.-G., Müller H. and Peters A., *J. Phys.: Conf. Ser.*, **723** (2016) 012050.
[8] Bidel Y., Zahzam N., Blanchard C., Bonnin A., Cadoret M., Bresson A., Rouxel D. and Lequentrec-Lalancette M. F., *Nat. Commun.*, **9** (2018) 627.
[9] Ménoret V., Vermeulen P., Le Moigne N., Bonvalot S., Bouyer P., Landragin A. and Desruelle B., *Sci. Rep.*, **8** (2018) 12300.
[10] Bongs K., Holynski M., Vovrosh J., Bouyer P., Condon G., Rasel E., Schubert C., Schleich W. P. and Roura A., *Nat. Rev. Phys.*, **1** (2019) 731.
[11] Dickerson S. M., Hogan J. M., Sugarbaker A., Johnson D. M. S. and Kasevich M. A., *Phys. Rev. Lett.*, **111** (2013) 083001.
[12] Sugarbaker A., Dickerson S. M., Hogan J. M., Johnson D. M. S. and Kasevich M. A., *Phys. Rev. Lett.*, **111** (2013) 113002.
[13] Hoth G. W., Pelle B., Riedl S., Kitching J. and Donley E. A., *Appl. Phys. Lett.*, **109** (2016) 071113.
[14] Chen Y.-J., Hansen A., Hoth G. W., Ivanov E., Pelle B., Kitching J. E. and Donley E. A., *Phys. Rev. Appl.*, **12** (2019) 014019.
[15] Chen Y.-J., Hansen A., Shuker M., Boudot R., Kitching J. E. and Donley E. A., arXiv:2005.11929 (2020).
[16] Cheinet P., Canuel B., Pereira Dos Santos F., Gauguet A., Yver-Leduc F. and Landragin A., *IEEE Trans. Instrum. Meas.*, **57** (2008) 1141.

[17] BARRETT B., GOMINET P.-A., CANTIN E., ANTONI-MICOLLIER L., BERTOLDI A., BATTELIER B., BOUYER P., LAUTIER J. and LANDRAGIN A., in *Proceedings of the International School of Physics "Enrico Fermi,"* Course 188, *"Atom Interferometry"*, edited by TINO G. M. and KASEVICH M. A. (SIF, Bologna, and IOS Press, Amsterdam) 2014, p. 493.

[18] AVINADAV C., YANKELEV D., SHUKER M., FIRSTENBERG O. and DAVIDSON N., *Phys. Rev. A*, **102** (2020) 013326.

[19] GOODWIN E. P. and WYANT J. C., *Field Guide to Interferometric Optical Testing* (SPIE, Bellingham) 2006.

[20] SCHREIBER H. and BRUNING J. H., in *Optical Shop Testing*, edited by MALACARA D. (John Wiley & Sons, Hoboken) 2007.